Inorganic Chemistry

Article

pubs.acs.org/IC

Role of π-Acceptor Effects in Controlling the Lability of Novel Monofunctional Pt(II) and Pd(II) Complexes: Crystal Structure of [Pt(tripyridinedimethane)Cl]Cl

Biljana Petrović,[†] Živadin D. Bugarčić,*[,†] Anne Dees,[‡] Ivana Ivanović-Burmazović,[‡] Frank W. Heinemann,[‡] Ralph Puchta,[‡] Stephan N. Steinmann,[§] Clemence Corminboeuf,[§] and Rudi van Eldik*[,‡]

[†]Faculty of Science, University of Kragujevac, Radoja Domanovica 12, P.O. Box 60, 34000 Kragujevac, Serbia

[‡]Inorganic Chemistry, Department of Chemistry and Pharmacy, University of Erlangen-Nürnberg, Egerlandstrasse 1, 91058 Erlangen, Germany

[§]Laboratory for Computational Molecular Design, Institute of Chemical Sciences and Engineering, Ecole Polytechnique Fédérale de Lausanne, EPFL ISC LCMD, CH-1015 Lausanne, Switzerland

Supporting Information

ABSTRACT: The kinetics and mechanism of substitution reactions of novel monofunctional $[Pt(tpdm)Cl]^+$ and $[Pd(tpdm)Cl]^+$ complexes (where tpdm = tripyridinedimethane) and their aqua analogues with thiourea (tu), L-methionine (L-met), glutathione (GSH), and guanosine-5′-monophosphate (5′-GMP) were studied in 0.1 M $NaClO_4$ at pH = 2.5 (in the presence of 10 mM NaCl for reactions of the chlorido complexes). The reactivity of the investigated nucleophiles follows the order tu > L-met > GSH > 5′-GMP. The reported rate constants showed the higher reactivity of the Pd(II) complexes as well as the higher reactivity of the aqua complex than the corresponding chlorido complex. The negative values reported for the activation entropy as well as the activation volume confirmed an associative substitution mode. In addition, the molecular and crystal structure of [Pt(tpdm)Cl]Cl was determined by X-ray crystallography. The compound crystallizes in a monoclinic space group $C2/c$ with two independent molecules of the complex and unit cell dimensions of a = 38.303(2) Å, b = 9.2555(5) Å, c = 27.586(2) Å, β = 133.573(1)°, and V = 7058.3(8) Å^3. The cationic complex $[Pt(tpdm)Cl]^+$ exhibits square-planar coordination around the Pt(II) center. The lability of the $[Pt(tpdm)Cl]^+$ complex is orders of magnitude lower than that of $[Pt(terpyridine)Cl]^+$. Quantum chemical calculations were performed on the $[Pt(tpdm)Cl]^+$ and $[Pt(terpyridine)Cl]^+$ complexes and their reactions with thiourea. Theoretical computations for the corresponding Ni(II) complexes clearly demonstrated that π-back-bonding properties of the terpyridine chelate can account for acceleration of the nucleophilic substitution process as compared to the tpdm chelate, where introduction of two methylene groups prevents such an effective π-back bonding.

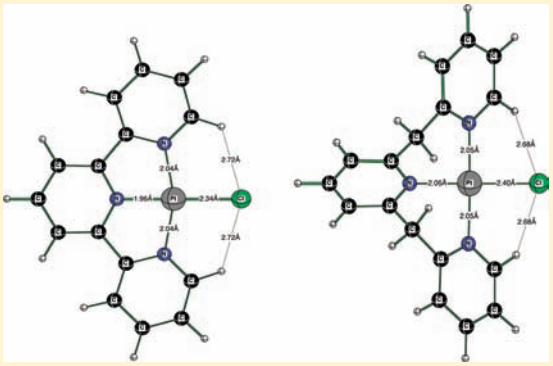

INTRODUCTION

Nucleophilic substitution reactions of square-planar d^8 complexes of Pt(II) and Pd(II) have received much attention over the last few decades.[1,2] Some Pt(II) complexes, like cisplatin, carboplatin, and oxaliplatin, are of special interest because of their application as antitumor drugs. Recently, there have been many efforts to design nonclassical platinum complexes, such as orally active Pt(IV) complexes, sterically hindered Pt(II) complexes, polynuclear Pt(II) and binuclear Pt(II) and Pd(II) complexes, sulfur-containing platinum complexes, etc., that gave better results in the treatment of tumors.[3−7] The interaction of Pt(II) complexes with sulfur-containing biomolecules, such as L-cysteine, L-methionine, and glutathione, has been associated with negative phenomena such as nephrotoxicity, gastrointestinal toxicity, ototoxicity, cardiotoxicity, and neurotoxicity.[6,8]

For mechanistic studies on the action of Pt(II) antitumor drugs, their Pd(II) analogues are usually good model compounds because they exhibit a 10^4−10^5-fold higher reactivity whereas their structural and equilibrium behavior is almost similar.[9] Also, coordination compounds of Pd(II) and Pt(II) with tridentate nitrogen-donor ligands, such as diethylenetriamine (dien), bis(2-pyridylmethyl)-amine (bpma), and 2,2′:6′,2″-terpyridine (terpy), provide very useful substrates for study of the substitution behavior of square-planar complexes. These tridentate ligands form very stable mononuclear complexes with Pd(II) and Pt(II) even under acidic conditions.

During the past two decades we developed a strong interest in the steric and electronic tuning of the lability of model

Received: August 18, 2011
Published: January 20, 2012

   dx.doi.org/10.1021/ic201807a | Inorg. Chem. 2012, 51, 1516−1529

square-planar Pt(II) and Pd(II) complexes and the influence this could have on the interaction of such complexes with biorelevant nucleophiles and DNA building blocks. We could, for instance, show how steric hindrance through introduction of methyl and ethyl substituents on the tridentate R_5dien chelate slowed down the substitution rate of a series of $[Pd(R_5dien)Cl]^+$ complexes by up to 6 orders of magnitude without having an affect on the nature of the underlying substitution mechanism that remained associative throughout the series of complexes.[10] On the other hand, introduction of electronic effects through systematic displacement of amine by pyridine donor groups on going from $[Pt(dien)Cl]^+$ to $[Pt(terpy)Cl]^+$ complexes resulted in an increase in the substitution rate of up to 4 orders of magnitude.[11] This was accounted for in terms of effective π-back bonding of the in-plane pyridine moieties with the nonbonding d electrons that lead to an increase in the electrophilicity of the metal center and stabilized the formation of a five-coordinate transition state during an associative ligand substitution process. In this way steric hindrance could decrease the lability of Pd(II) complexes to reach that of closely related Pt(II) complexes, whereas electronic effects could increase the lability of Pt(II) complexes to reach that of closely related Pd(II) complexes.[10,11] In principle, such tuning of the lability of antitumor-related Pt(II) complexes could play an important role in the development of a new series of complexes designed for treatment of specific types of tumors employing alternative treatment therapies.

In earlier studies we performed systematic kinetic analyses of the reactions of different chelated complexes of Pt(II) and Pd(II) with series of biorelevant nucleophiles and found the highest reactivity for the terpyridine complexes throughout the series. This could be accounted for in terms of the mentioned π-back-bonding effect of the aromatic in-plane-coordinated pyridine ligands. We have now synthesized the corresponding complexes for the tpdm (tripyridinedimethane) chelate in which a methylene group bridges the adjacent pyridine groups. Due to the tetrahedral arrangement around the methylene groups the pyridine ligands are forced to be out of plane with the metal center, which should have a significant effect on their π-back-bonding ability and as a result the lability of the synthesized complexes. This was indeed found to be the case. The reported crystal structure of the [Pt(tpdm)Cl]Cl compound clearly shows the deviations from the planar arrangement found for the corresponding terpyridine compound. DFT computations were performed in an effort to account for the orders of magnitude difference in the reactivity of the tpdm and terpy complexes.

We further studied the kinetics and mechanism of substitution reactions of the novel monofunctional $[Pt(tpdm)Cl]^+$ and $[Pd(tpdm)Cl]^+$ complexes and their aquated analogues with thiourea (tu), L-methionine (L-met), glutathione (GSH), and guanosine-5′-monophosphate (5′-GMP). The entering ligands were investigated because of their different nucleophilicity, steric hindrance, binding properties, and biologically relevance. Thiourea is a very useful nucleophile since it combines the ligand properties of thiolates (σ-donor) and thioethers (σ-donor, π-acceptor).[12−14] In addition, there are several reasons to study the reactions with the other three nucleophiles. As mentioned before, reactions with 5′-GMP are used as a model for binding to DNA, whereas the sulfur-containing biomolecules (L-met and GSH) play an important role in toxic side effects in the antitumor action of Pt(II) complexes. The structures of the studied complexes and nucleophiles are summarized in Scheme 1.

EXPERIMENTAL SECTION

Chemicals and Ligands. The ligands L-methionine, glutathione, guanosine-5′-monophosphate sodium salt, and thiourea were obtained from Fluka and Acros Organics and used without further purification. Potassium tetrachloridoplatinate(II) (K_2PtCl_4) and potassium tetrachlorido−palladate(II) (K_2PdCl_4) were purchased from Strem Chemicals. Cyclooctadien (Across Organics) was used in the stepwise preparation of the novel complexes. The chelate tripyridinedimethane (tpdm) was synthesized according to a published procedure.[15] All other chemicals were of the highest purity commercially available. Ultrapure water was used in the kinetic as well as spectrophotometric measurements. Nucleophile stock solutions were prepared shortly before use by dissolving the chemicals. The ionic strength of all solutions was adjusted to 0.10 M with $NaClO_4$. Ten millimolar NaCl was added to the aqueous solutions of the chlorido complexes to prevent their hydrolysis.

Synthesis of Compounds. [Pt(tpdm)Cl]Cl and [Pd(tpdm)Cl]Cl were prepared starting from K_2PtCl_4 and K_2PdCl_4, respectively. To an aqueous solution of K_2PtCl_4 (1 mmol) an equimolar concentration of cyclooctadiene (COD) was added and stirred for 1 h. The weakly soluble $[Pt(COD)Cl_2]$ complex was filtered off, dried, and mixed with an equivalent concentration of tpdm in a methanol/water (50/50, v/v) mixture. The suspension was steered for a few hours, and the temperature was kept at about 50 °C. After cooling to room temperature, the solution was left in ice overnight. The yellow precipitate was separated from the solution, recrystallized from water, and characterized by X-ray diffraction, elemental analysis, and UV and IR spectroscopies (Figures S1 and S2, Supporting Information). Anal. Calcd for $PtN_3C_{17}H_{15}Cl_2$: H, 2.87; C, 38.2; N, 7.97. Found: H, 2.66; C, 38.3; N, 7.13. λ_{max} compl./nm 267.0; ν_{max}/cm^{-1} 764 (Pt−N), 1469 (C−N), 1607 (C═N), 3400 (O−H).

The same procedure was used for synthesis of the corresponding Pd(II) complex. After obtaining a dark yellow powder, the compound was characterized by elemental analysis and UV and IR spectroscopies (Figures S3 and S4, Supporting Information). Anal. Calcd for $PdN_3C_{17}H_{15}Cl_2$: H, 3.42; C, 46.53; N, 9.58. Found: H, 3.92; C, 44.07; N, 8.37. λ_{max} compl./nm 265.1; ν_{max}/cm^{-1} 786 (Pt−N), 1454 (C−N), 1591 (C═N), 3400 (O−H).

The aqua complexes $[Pt(tpdm)(H_2O)]^{2+}$ and $[Pd(tpdm)(H_2O)]^{2+}$ were prepared starting from the corresponding chlorido complexes. Conversion was performed by addition of a slight excess of $AgClO_4$ to a solution of the chlorido complex and stirring for 3 h at 50 °C. The white precipitate that formed (AgCl) was filtered off using a Millipore filtration unit, and the solution was diluted. In order to ensure that the resulting solution was free of Ag^+ ions, the pH of the solution was increased to 11 by addition of small amounts of 0.1 M NaOH solution. This led to formation of brown silver oxide (from the excess silver perchlorate), which was then removed with a Millipore filter, and the pH of the remaining solution was adjusted to pH 2.5 with perchloric acid. UV−vis and IR spectra of the aqua complexes are reported in Figures S5−S8, Supporting Information. Addition of chloride to the solution of the aqua complexes immediately resulted in reformation of the chlorido species as observed from the UV−vis spectral changes. Since it is well known that perchlorate ions do not coordinate to Pt(II) and Pd(II) in aqueous solution,[16] the kinetics of the complex-formation reactions were studied in perchlorate medium.

Instrumentation. Chemical analyses were performed on a Carlo Erba Elemental Analyzer 1106. IR spectra were recorded on Perkin-Elmer Spectrum One FTIR spectrometer, whereas UV−vis spectra were recorded on Shimadzu UV 250 and Hewlett-Packard 8452A diode-array spectrophotometers in thermostatted, 1.00 cm quartz Suprasil cells. Kinetic measurements on the Pd(II) complex were carried out on an Applied Photophysics SX.18MV stopped-flow instrument coupled to an online data acquisition system. For reactions of the Pt(II) complex, a Perkin-Elmer Lamda 35 spectrophotometer was used. Experiments at elevated pressure (up to 130 MPa) were performed on a homemade high-pressure stopped-flow unit[17] attached to an online data acquisition system with which the kinetic traces could be evaluated using the OLIS KINFIT (Bogart, GA) set of programs. The temperature was controlled throughout all kinetic experiments to ±0.1 °C.

dx.doi.org/10.1021/ic201807a | Inorg. Chem. 2012, 51, 1516−1529

Scheme 1. Schematic Structures of Studied Complexes and Nucleophiles

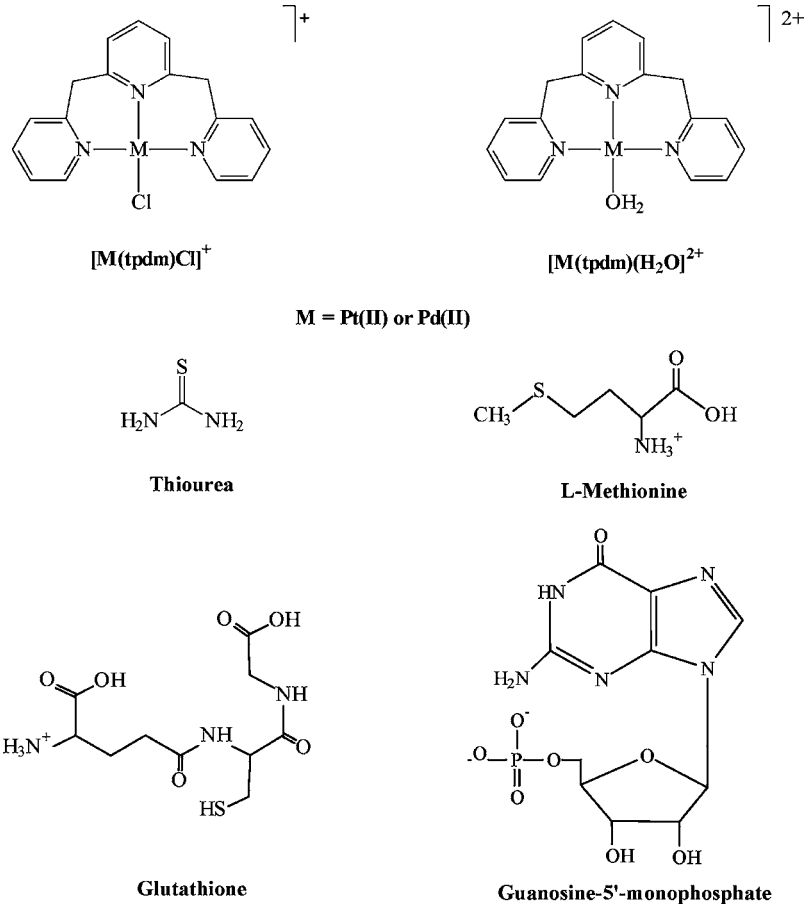

Kinetic Measurements. Substitution reactions of the novel monofunctional Pt(II) and Pd(II) complexes with the nucleophiles L-methionine, glutathione, 5′-GMP, and thiourea were studied spectrophotometrically by following the change in absorbance at suitable wavelengths as a function of time. Spectral changes resulting from mixing the complex and nucleophile solutions were recorded over the wavelength range 200−400 nm to establish a suitable wavelength at which kinetic measurements could be performed.

Substitution reactions of $[Pd(tpdm)Cl]^+$ and $[Pd(tpdm)(H_2O)]^{2+}$ were initiated by mixing equal volumes of complex and ligand solutions directly in the stopped-flow instrument and followed for at least eight half-lives. The substitution process was monitored as the change in absorbance with time under pseudo-first-order conditions (working wavelengths are given in Tables S1−S7, Supporting Information). All kinetic runs could be fitted to a single-exponential function.

Substitution reactions of $[Pt(tpdm)Cl]^+$ and $[Pt(tpdm)(H_2O)]^{2+}$ were started by mixing 0.3 mL of the complex solution with 2.7 mL of nucleophile solution in a quartz cuvette. The concentration of the nucleophile solution was always high enough (at least a 10-fold excess) to provide pseudo-first-order conditions. The kinetic traces also gave an excellent fit to a single-exponential function.

The observed pseudo-first-order rate constants, k_{obsd}, were calculated as the average value from 4−6 independent kinetic runs using the program Origin 6.1. Experimental data are reported in Tables S1−S7, Supporting Information.

All experiments with the chlorido complexes were studied in the presence of 10 mM NaCl to prevent spontaneous hydrolysis. This concentration of NaCl was based on kinetic measurements performed as a function of NaCl concentration for the reaction of $[Pt(tpdm)(H_2O)]^{2+}$ with thiourea (see Table S8, Supporting Information).

The pressure dependence of the observed rate constant for reaction between $[Pd(tpdm)Cl]^+$ and glutathione was studied at 10 °C in the range 0.1−130 MPa. This reaction was also followed under pseudo-first-order conditions with an excess of the nucleophile. High-pressure kinetic data are reported in Table S9 (Supporting Information).

Quantum Chemical Computations. We performed B3LYP/LANL2DZp hybrid density functional computations on $[Pt(terpy)Cl]^+$ and $[Pt(tpdm)Cl]^+$, i.e., with pseudopotentials on the heavy elements and the valence basis set augmented with polarization functions.[18,19] While optimizing the structures no other constraints than symmetry were applied. In addition, the resulting structures were characterized as minima by computation of vibrational frequencies. The relative energies were corrected for zero-point vibrational energies (ZPE) throughout. The GAUSSIAN suite of programs was used.[20] The influence of the bulk solvent was evaluated via single-point computations using the CPCM[21] formalism, i.e., B3LYP(CPCM)/LANL2DZp//B3LYP/-LANL2DZp and water as solvent.

In an effort to gain further insight into the role of π-back-bonding in such complexes, the corresponding Ni monocationic complexes (closed shell) were optimized at the B3LYP[18a,b]/LANL2DZ[18e] level. The property computations for the free ligands were based on the same geometry as for the complexes. The computational strategy[22] combined Mo et al.'s block-localized wave function (BLW) scheme[23,24] with Kutzelnigg's IGLO methodology[25] to analyze the nucleus-independent chemical shifts (i.e., NICS-based indices)[26,27] of model reference species with "chemically noninteracting" (disabled) double bonds.

Electronic structures used in the property computations employed a modified version of GAMESS-US (release 2008)[28,29] interfaced with the BLW module. A modified version of the deMon-MASTER code[30] that computes the NMR parameters by numerical integration for both the delocalized (standard) and the electronic structures with non-interacting π bonds was employed. The Pipek−Mezey MO localization and the chemical shift dissection were based on the σ/π symmetry. Chemical shifts were improved by the LOC1 ad hoc correction for

dx.doi.org/10.1021/ic201807a | Inorg. Chem. 2012, 51, 1516−1529

virtual orbitals.[31] The (BLW)-NICS$_{zzz}$ values were computed at the (BLW-)PW91[32]/IGLO-III level (partially uncontracted def2-QZVPP basis set without f and g function for Ni). A dense 140/1202 (or even 200/1202 in certain cases) Euler−Maclaurin−Lebedev[33,34] was used in the SCF procedure. Delocalization energies were computed at the PW91/IGLO-III level and correspond to the difference between the energy of the canonical (standard) electronic structure and the energy of the localized state computed using the block-localized wave function method. Note that the current formalism is incompatible with use of the pseudopotential and hence has been restricted to the nickel complex.

X-ray Crystallography. Intensity data for a crystal of [Pt(tpdm)-Cl]Cl·1.25H_2O with approximate dimensions of 0.15 × 0.10 × 0.08 mm were collected on a Bruker Kappa APEX 2 IμS Duo diffractometer using Mo Kα radiation (QUAZAR focusing Montel optics, λ = 0.71073 Å) at 150 K. Lorentz and polarization corrections as well as a semiempirical absorption correction based on multiple scans were applied (SADABS 2.11, Bruker AXS, 2009). The structure was solved by direct methods and refined using full-matrix least-squares procedures on F^2 (SHELXTL NT 6.12, Bruker AXS, 2002). The asymmetric unit contains two independent molecules of [Pt(tmpd)Cl]Cl and a total of 2.5 water molecules. One of the chloride anions is disordered over two crystallographic sites with 50% occupancy each. One site of the solvate water molecules is occupied by approximately 50% only. The positions of the hydrogen atoms of the solvate water molecules were derived from a difference Fourier synthesis and not refined. All other hydrogen atoms were placed in positions of optimized geometry. The isotropic displacement parameters of all H atoms were tied to those of their corresponding carrier atoms by a factor of 1.2 or 1.5.

CCDC 838701 for [Pt(tpdm)Cl]Cl·1.25H_2O contains the supplementary crystallographic data. These data can be obtained free of charge from The Cambridge Crystallographic Data Centre via www.ccdc.cam.ac.uk/data_request/cif. Crystal data and structure refinement details for [Pt(tpdm)Cl]Cl·1.25H_2O are summarized in Table 1.

Table 1. Crystal Data and Structure Refinement Details for [Pt(tpdm)Cl]Cl·1.25H_2O

empirical formula	$C_{34}H_{35}Cl_4N_6O_{2.5}Pt_2$
fw	1099.66 g/mol
temp.	150(2) K
wavelength	0.71073 Å
cryst syst, space group	monoclinic, $C2/c$
unit cell dimens	a = 38.303(2) Å
	b = 9.2555(5) Å
	c = 27.586(2) Å
	α = 90°
	β = 133.573(1)°
	γ = 90°
vol.	7085.3(8) Å^3
Z, calcd density	8, 2.062 Mg/m^3
abs coeff	8.234 mm^{-1}
F(000)	4200
cryst size	0.15 × 0.10 × 0.08 mm
theta range for data collection	2.32−27.10°
limiting indices	$-34 \le h \le 48$
	$-11 \le k \le 11$
	$-34 \le l \le 19$
reflns collected/unique	21 252/7544 [R(int) = 0.0361]
completeness to theta = 25.00	97.6%
abs corr	semiempirical from equivalents
max and min transmission	0.746 and 0.614
data/restraints/params	7544/9/449
goodness-of-fit on F^2	1.026
final R indices [$I > 2\sigma(I)$]	R_1 = 0.0304, wR_2 = 0.0716
R indices (all data)	R_1 = 0.0407, wR_2 = 0.0758
largest diff. peak and hole	1.641 and −0.864 e Å^{-3}

RESULTS AND DISCUSSION

Crystal Structure of]Pt(tpdm)Cl]Cl·1.25H_2O. The molecular structure of [Pt(tpdm)Cl]Cl was confirmed by X-ray crystal structure determination and is shown in Figures 1 and 2.

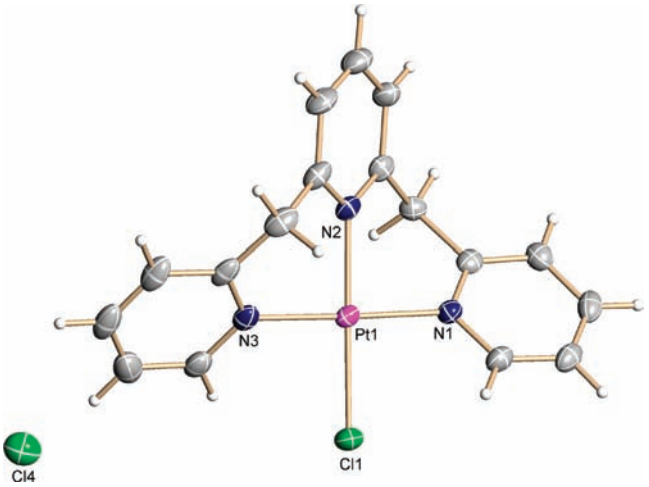

Figure 1. Molecular structure of the [Pt(tpdm)Cl]Cl compound in crystals of [Pt(tpdm)Cl]Cl·1.25H_2O (50% probability ellipsoids, second independent complex salt and solvate water molecules omitted for clarity).

Selected bond lengths and angles are given in Table 2. As can be seen from Figure 1, the tridentate tpdm ligand is coordinated to the Pt(II) center by the nitrogen donors of the three pyridine rings while the fourth position is occupied by a chloride ion. The Pt−N2 distance of 2.005(5) Å is marginally shorter than Pt−N1 (2.015(4) Å) and Pt−N3 (2.010(5) Å). The coordination geometry of the complex is square planar with slight distortions from ideal values according to the observed N−Pt−N and N−Pt−Cl angles (see Table 2). A least-squares plane calculated through the central platinum atom and the four donor atoms reveals a maximum deviation from the ideal plane of 0.013(2) Å for N2. All three pyridine ring planes are tilted with respect to this central plane by approximately 40° (ring N1 by 41.3(3)°, ring N2 by 40.6(2)°, and ring N3 by 39.6(2)°). The asymmetric unit contains two independent molecules of [Pt(tpdm)Cl]Cl with basically the same metric parameters and conformation for the complex cation and a total of 2.5 water molecules. The crystal packing is characterized by a number of hydrogen bonds linking the cations with oxygen and chloride ions (Table S10, Supporting Information).

In connection with the bond distances obtained for the [Pt(tpdm)Cl]Cl compound, it can be seen that the presence of two methylene groups in the structure of the tpdm chelate strongly increases its flexibility and simultaneously decreases its lability in comparison with the [Pt(terpy)Cl]Cl compound (see the next section). The very strong interactions between the Pt(II) center and the terpy ligand result in a significantly shorter Pt−N2 bond distance of 1.940 Å, whereas the Pt−Cl bond has a distance of 2.296 Å in [Pt(terpy)Cl]Cl.[35] In the case of [Pt(tpdm)Cl]Cl the Pt−N2 bond length is 2.005(5) Å, while the Pt−Cl distance amounts to 2.289(2) Å. These differences in bond lengths contribute to the fact that the trans effect of the coordinated tpdm ligand is much smaller than that of the terpy ligand (see further discussion).

Kinetic and mechanistic studies. We now report the results of kinetic studies on substitution reactions of the novel

dx.doi.org/10.1021/ic201807a | Inorg. Chem. 2012, 51, 1516−1529

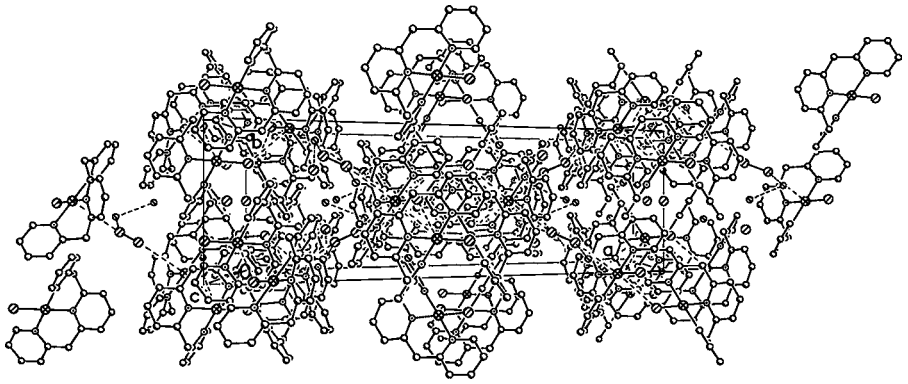

Figure 2. Crystal packing of $[Pt(tpdm)Cl]Cl{\cdot}1.25H_2O$. View along the crystallographic *c* axis. Dotted lines indicate hydrogen bonds.

Table 2. Selected Bond Lengths [Angstroms] and Angles [degrees] for $[Pt(tpdm)Cl]Cl{\cdot}1.25H_2O$

Pt(1)−N(2)	2.005(5)
Pt(1)−N(3)	2.010(5)
Pt(1)−N(1)	2.015(4)
Pt(1)−Cl(1)	2.289(2)
N(2)−Pt(1)−N(3)	89.6 (2)
N(2)−Pt(1)−N(1)	88.8(2)
N(3)−Pt(1)−N(1)	178.4(2)
N(2)−Pt(1)−Cl(1)	178.9(2)
N(3)−Pt(1)−Cl(1)	90.7(2)
N(1)−Pt(1)−Cl(1)	90.8(2)

square-planar, monofunctional $[Pt(tpdm)Cl]^+$ and $Pd(tpdm)Cl]^+$. These complexes contain the tridentate tpdm chelate as a spectator ligand, whereas chloride or water are the labile ligands. All reactions were followed in 0.1 M $NaClO_4$ at pH = 2.5. This pH was selected in order to prevent possible formation of hydroxo complexes.

The different substitution routes of the chlorido and aqua square-planar complexes are summarized in Scheme 2.

Scheme 2. Overall Reaction Scheme for Substitution Reactions of $[M(tpdm)Cl]^+$

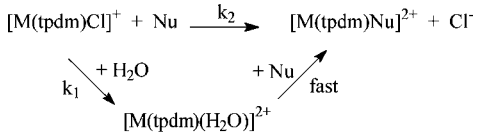

M = Pt(II) or Pd(II)
Nu = Tu, L-Met, GSH or 5'-GMP

According to Scheme 2, substitution of the chlorido complex proceeds according to two parallel pathways,[36] viz. direct nucleophilic attack characterized by the rate constant k_2 and an aquation pathway during which a very labile aqua complex is formed in the rate-determining step characterized by the rate constant k_1. The produced aqua complex usually reacts rapidly with the nucleophile to form $[M(tpdm)Nu]^{2+}$. The selected nucleophiles are all very strong donor ligands, such that a reverse reaction by which they are replaced by chloride does not occur. Under pseudo-first-order conditions these rate constants can be determined from the slope (k_2) and intercept (k_1) of plots of k_{obsd} vs nucleophile concentration according to eq 1.

$$k_{obsd} = k_1 + k_2[Nu] \quad (1)$$

By way of example, Figure 3 shows the typical spectral changes observed for reaction between $[Pd(tpdm)(H_2O)]^{2+}$ and

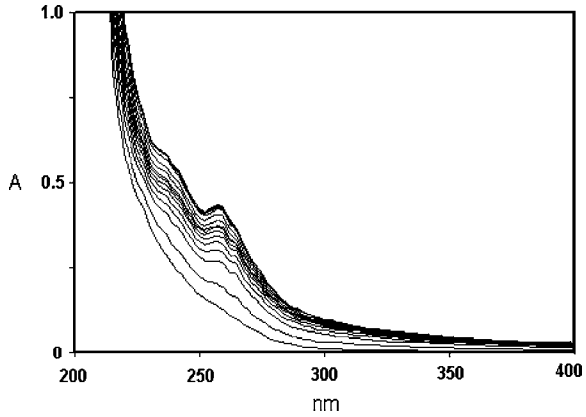

Figure 3. UV−vis spectra recorded as a function of time for reaction between $[Pd(tpdm)Cl]^+$ and glutathione at 298 K in 0.1 M $NaClO_4$, pH = 2.5, and 10 mM NaCl.

glutathione from which the substitution rate constants were calculated. Other examples for the studied reactions are presented in Figures S9−S12 (Supporting Information). Typical experimental results for substitution reactions of $[Pd(tpdm)Cl]^+$ and $[Pt(tpdm)Cl]^+$ with different nucleophiles are reported in Figures 4 and 5, and the obtained values for k_1 and k_2 are summarized in Table 3. At the start of the work the influence of different NaCl concentrations (between 0.2 and 10 mM) on the observed rate constants for the substitution reaction between $[Pd(tpdm)(H_2O)]^{2+}$ and thiourea was investigated. The results reported in Figure 6 clearly indicate that an increase in the chloride concentration up to 5 mM NaCl decreases the value of the pseudo-first-order rate constant, and a limiting value is reached at this chloride concentration level. This is due to a shift in the equilibrium from the labile aqua complex to the inert chlorido complex. Therefore, all substitution reactions of the Pt(II) and Pd(II) chlorido complexes were studied in the presence of 10 mM NaCl to prevent the parallel aquation reaction completely.

In Scheme 3 the reversible substitution reaction of the aqua complexes is summarized. Substitution of the monofunctional aqua complexes of Pt(II) and Pd(II) involves a reversible process characterized by the rate constants k_2 for direct

dx.doi.org/10.1021/ic201807a | *Inorg. Chem.* 2012, 51, 1516−1529

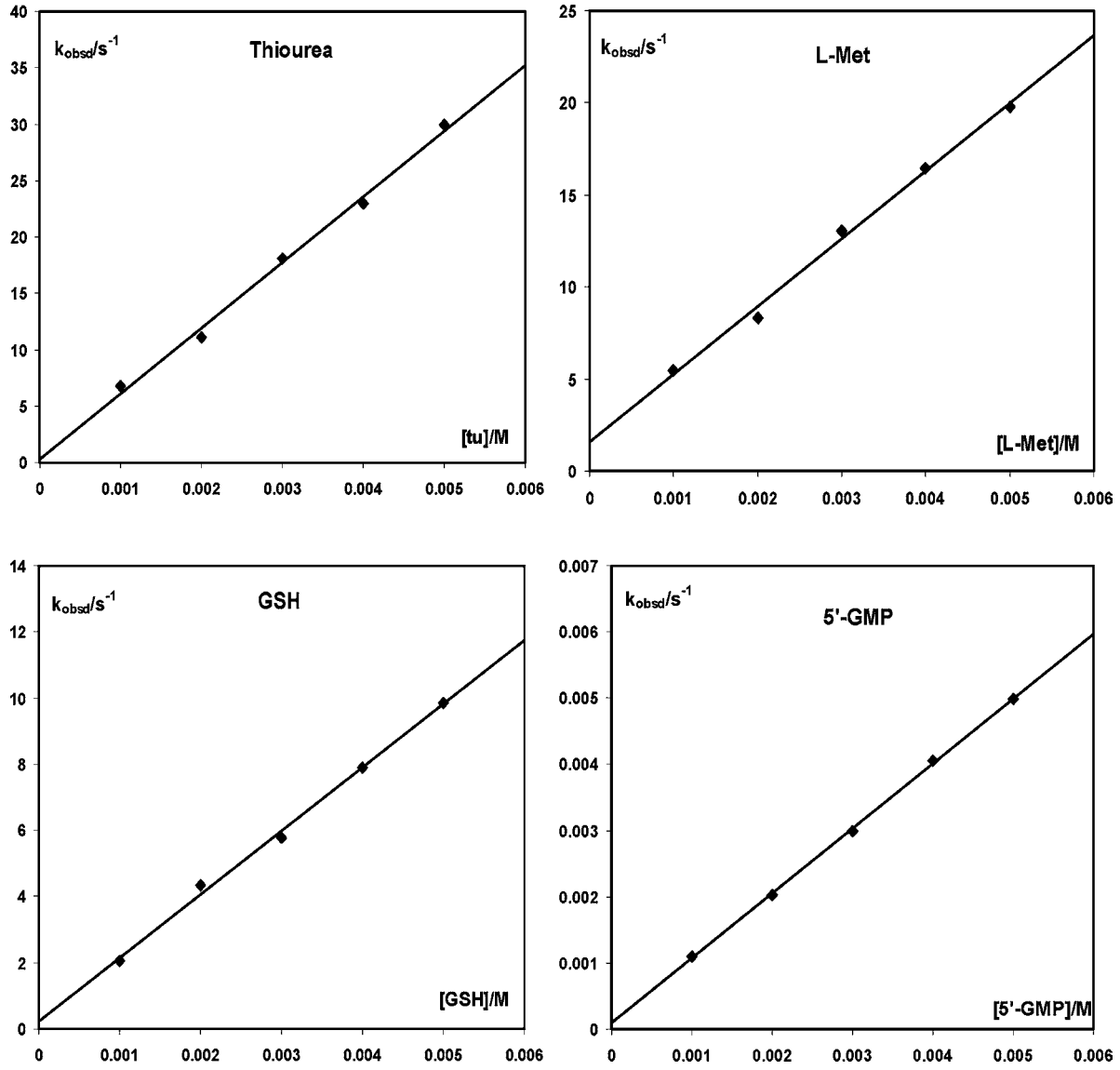

Figure 4. Pseudo-first-order rate constants, k_{obsd}, as a function of entering nucleophile concentration for substitution reactions of $[Pd(tpdm)Cl]^+$ at 298 K in 0.1 M $NaClO_4$, pH = 2.5, and 10 mM NaCl.

Scheme 3

$$[M(tpdm)(H_2O)]^{2+} + Nu \underset{k_{-2}}{\overset{k_2}{\rightleftharpoons}} [M(tpdm)Nu]^{2+} + H_2O$$

M = Pt(II) or Pd(II)
Nu = Tu, L-Met, GSH or 5'-GMP

substitution of coordinated water by the nucleophile and k_{-2} for the reverse aquation reaction. Under pseudo-first-order conditions the values of these rate constants could be determined from the slopes and intercepts of plots of k_{obsd} vs nucleophile concentration according to eq 2.

$$k_{obsd} = k_{-2} + k_2[Nu] \quad (2)$$

Typical experimental results for these reactions are shown in Figures 7 and 8, and the calculated values for the rate constants are also included in Table 3. To confirm that these complexes follow an associative substitution mode characteristic for square-planar complexes, some of the reactions were studied at different temperatures in the range 288−308 K. The calculated values for the enthalpy and entropy of activation are also included in Table 3. The reported activation entropy values are all significantly negative in line with an associative substitution mechanism. In addition, reaction between $[Pd(tpdm)Cl]^+$ and glutathione was studied as a function of pressure at 10 °C (see Table S9, Supporting Information). The plot of ln k_{obsd} vs pressure was linear and resulted in a negative value for the volume of activation, viz. $\Delta V^{\ddagger} = -9.1 \pm 0.3$ cm^3 mol^{-1}, which further supports the associative nature of the substitution mechanism.

On the basis of the results summarized in Table 3, it can be concluded that selected nucleophiles are very good entering ligands for substitution reactions of the studied monofunctional complexes. The reactivity order follows the trend tu > L-met > GSH > 5′-GMP at pH 2.5. Thiourea is a small ligand as compared to the other three ligands, and it has a sulfur donor atom with a very high nucleophilicity. L-met shows a slightly lower reactivity, where the positive inductive effect of the methyl group increases the nucleophilicity of the sulfur donor

dx.doi.org/10.1021/ic201807a | Inorg. Chem. 2012, 51, 1516−1529

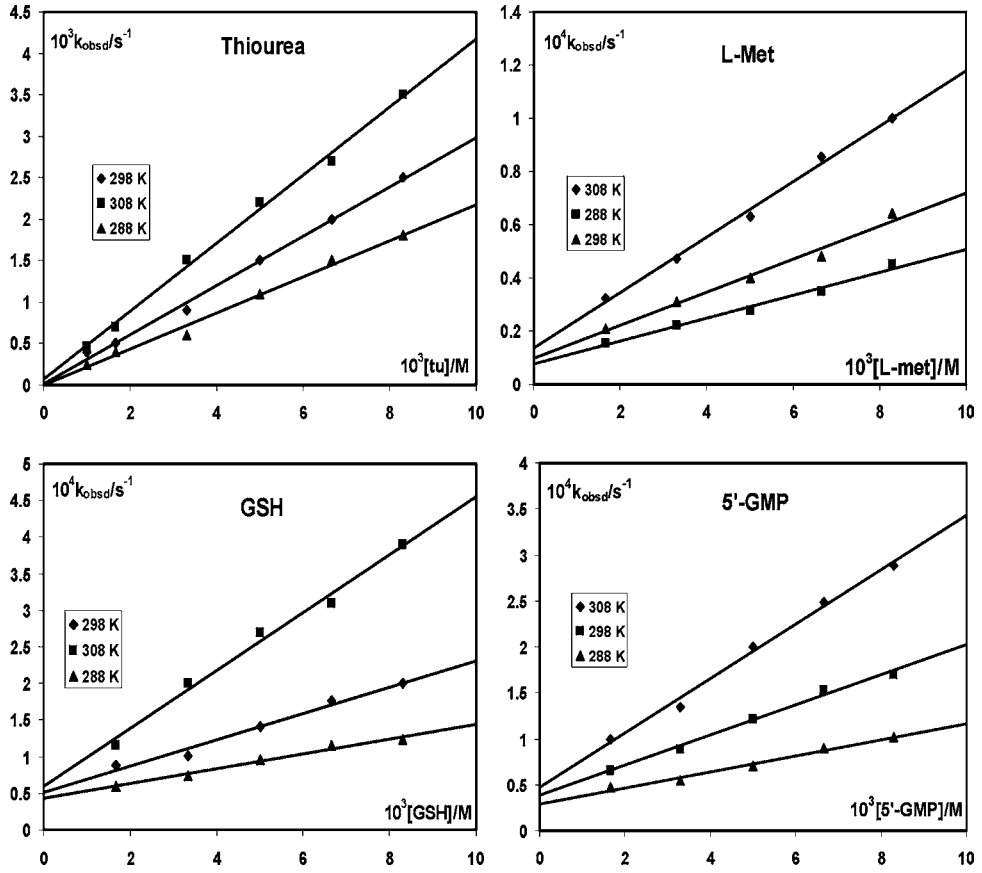

Figure 5. Pseudo-first-order rate constants, k_{obsd}, as a function of entering nucleophile concentration and temperature for substitution reactions of $[Pt(tpdm)Cl]^{2+}$ in 0.1 M $NaClO_4$, pH = 2.5, and 10 mM NaCl.

Table 3. Rate Constants and Activation Parameters for Substitution Reactions of Some Pd(II) and Pt(II) Complexes at 298 K in 0.1 M $NaClO_4$ at pH = 2.5[a]

complex	ligand	$k_2/M^{-1}\ s^{-1}$	k_1/s^{-1}	$\Delta H_2^{\ddagger}$/kJ mol^{-1}	$\Delta S_2^{\ddagger}$/J K^{-1} mol^{-1}
$[Pd(tpdm)Cl]^+$	thiourea	$(5.8 \pm 0.2) \times 10^3$	0.37 ± 0.08	29 ± 3	-75 ± 8
	L-Met	$(3.7 \pm 0.2) \times 10^3$	1.56 ± 0.08		
	GSH	$(1.92 \pm 0.06) \times 10^3$	0.22 ± 0.02	27 ± 2	-90 ± 7
	5′-GMP	0.98 ± 0.01	$(9.1 \pm 0.9) \times 10^{-5}$	11 ± 2	-194 ± 8
$[Pt(tpdm)Cl]^+$	thiourea	$(12.1 \pm 0.1) \times 10^{-2}$	$(7.0 \pm 0.2) \times 10^{-4}$	31 ± 2	-156 ± 11
	L-Met	$(6.21 \pm 0.05) \times 10^{-2}$	$(9.9 \pm 0.3) \times 10^{-5}$	31 ± 3	-164 ± 9
	GSH	$(1.79 \pm 0.01) \times 10^{-2}$	$(5.2 \pm 0.8) \times 10^{-5}$	48 ± 4	-118 ± 13
	5′-GMP	$(1.63 \pm 0.04) \times 10^{-2}$	$(3.9 \pm 0.5) \times 10^{-5}$	43 ± 3	-136 ± 10
		$k_2/M^{-1}\ s^{-1}$	k_{-2}/s^{-1}	$\Delta H_2^{\ddagger}$/kJ mol^{-1}	$\Delta S_2^{\ddagger}$/J K^{-1} mol^{-1}
$[Pd(tpdm)(H_2O)]^{2+}$	thiourea	$(2.2 \pm 0.3) \times 10^4$	0.03 ± 0.01	21 ± 2	-90 ± 7
	L-Met	$(7.42 \pm 0.09) \times 10^3$	3.7 ± 0.3		
	5′-GMP	2.8 ± 0.1	$(3.7 \pm 0.3) \times 10^{-4}$	21 ± 3	-165 ± 10
$[Pt(tpdm)(H_2O)]^{2+}$	thiourea	$(3.0 \pm 0.1) \times 10^{-1}$	$(2.0 \pm 0.4) \times 10^{-5}$	21 ± 3	-185 ± 9
	L-Met	$(7.85 \pm 0.05) \times 10^{-2}$	$(4.0 \pm 0.1) \times 10^{-4}$	33 ± 2	-154 ± 7
	5′-GMP	$(3.87 \pm 0.04) \times 10^{-2}$	$(3.6 \pm 0.2) \times 10^{-4}$	59 ± 4	-74 ± 12

[a] 10 mM NaCl was added only for reactions of the chlorido complexes.

atom. This result is important since similar monofunctional complexes of Pt(II) and Pd(II) with tridentate terpyridine ligands do not react with thioethers.[37,38] This observation can be explained in terms of the steric effect of the terpyridine chelate, as the tridentate tpdm system is more flexible in comparison with terpyridine since the pyridine rings are now separated by a methylene group.

The tripeptide GSH is also a very good nucleophile for the $[Pd(tpdm)Cl]^+$ and $[Pt(tpdm)Cl]^+$ complexes. Under the conditions of the studied reactions only the COOH group of the GSH molecule is deprotonated (pK_{a1} = 2.05).[39] Thus, as mentioned before,[11c,f,38−42] the presence of hydrogen-bonding interactions between the thiol group and the deprotonated carboxylate group located in a suitable position could increase the nucleophilicity of the sulfur atom. These interactions are responsible for the remarkable high reactivity of the tripeptide glutathione in comparison with, for example, the free amino acid L-cysteine.[11c,f] GSH under the studied conditions is less

dx.doi.org/10.1021/ic201807a | Inorg. Chem. 2012, 51, 1516−1529

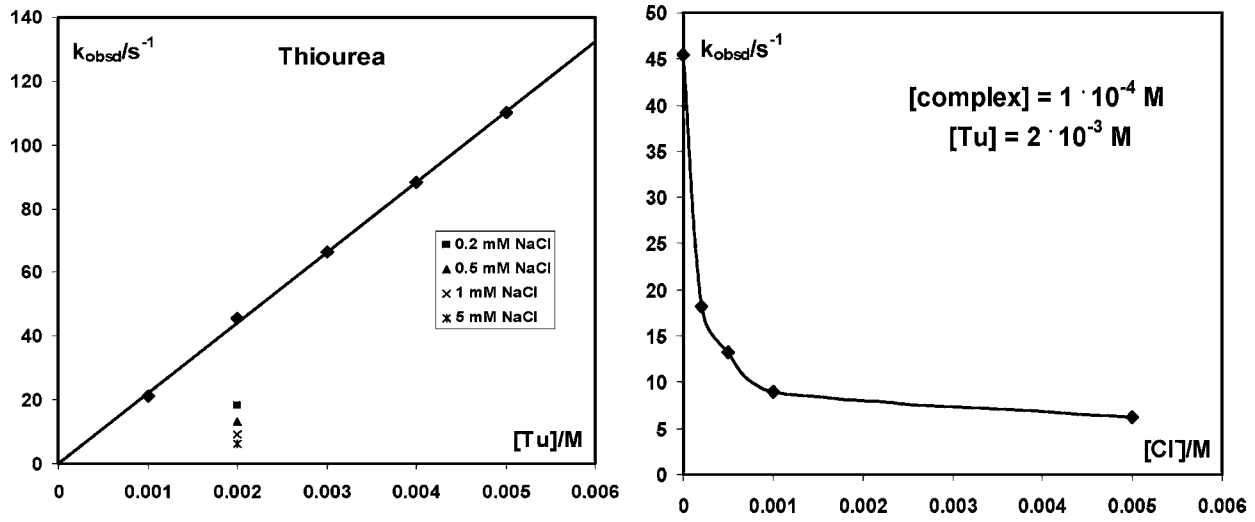

Figure 6. Influence of different chloride concentrations on the pseudo-first-order rate constant for reaction between $[Pd(tpdm)(H_2O)]^{2+}$ and thiourea at 298 K in 0.1 M $NaClO_4$ and pH = 2.5.

reactive than L-met because the sulfur atom is protonated at a pH of 2.5.[39] The employed nitrogen-donor ligand, 5′-GMP, reacts slowly with the investigated complexes. This fact can be explained by the difference in donor atom and by the bulkiness of the 5′-GMP molecule as compared to the other three ligands. It should be noted that the observed reactivity pattern could be quite different under physiological conditions due to deprotonation of the functional groups on some of these nucleophiles at higher pH.

The rate constants k_2 obtained for substitution of $[Pd(tpdm)Cl]^+$ and $[Pt(tpdm)Cl]^+$ show that direct nucleophilic attack is a dominant pathway in the overall substitution process, whereas the solvolytic rate constants k_1 are independent of the nature of the entering ligand and contribute little to the observed rate constants. This mode of substitution was also reported[11c,g,40−45] for other square-planar complexes of Pt(II) and Pd(II), which have an inert tridentate nitrogen-donor chelate and chloride ion as leaving group. From a comparison of the reported rate constants for reactions with the same nucleophile it can be seen that $[Pd(tpdm)Cl]^+$ reacts about 10^4−10^5 times faster than $[Pt(tpdm)Cl]^+$, which is within the general difference in reactivity of Pd(II) and Pt(II) complexes reported in the literature.[1,11c,e,41−45] Only in the case of 5′-GMP, this ratio is only ca. 60, which could be due to partial preassociation between the metal complex and the phosphate group in 5′-GMP before coordination to the N7 site.

Substitution reactions of $[Pd(tpdm)(H_2O)]^{2+}$ and $[Pt(tpdm)(H_2O)]^{2+}$ are reversible processes and characterized by rate constants for the forward reaction, k_2, and for the reverse reaction, k_{-2}. A comparison of the forward rate constants reveals the same order of ligand reactivity as found for the reactions of the corresponding chlorido complexes. Also, the remarkable higher reactivity (about 5 orders of magnitude) of the Pd(II) complex should be mentioned, except for reactions with 5′-GMP. The stability constants of the formed complexes were calculated from the ratio k_2/k_{-2}. The most stable complex is formed between $[Pd(tpdm)(H_2O)]^{2+}$ and thiourea, $K = 6.7 \times 10^5$ M^{-1}, whereas significantly lower values of ca. 10^3 M^{-1} exist for the other studied nucleophiles. On the other hand, Pt(II) analogues are less stable for the studied nucleophiles. The values for the complex with L-methionine and 5′-GMP are around 10^2 M^{-1}, while the complex with thiourea is more stable, $K = 1.5 \times 10^4$ M^{-1}. Thiourea is the smallest nucleophile and can form stable complexes with the studied metal ions enclosed by the nonplanar tridentate ligand compared to other more voluminous nucleophiles. From another point of view, the stability of the formed complexes could be connected with electronic effects of the chelates, viz. their σ-donor and π-acceptor characteristics.

The results reported in Table 3 show as expected[36] that $[Pd(tpdm)(H_2O)]^{2+}$ and $[Pt(tpdm)(H_2O)]^{2+}$ have a higher reactivity than the corresponding chlorido complexes since the coordinated water molecule is more labile and a better leaving group than chloride. Notably, the effect is not as large as found in other cases,[36] which indicates that bond formation to form a five-coordinate intermediate is more important than bond breakage with the leaving nucleophile for both the aqua and the chloride complexes. The higher electrophilicity of the metal center in the case of the aqua complex accounts for the faster reactions than observed for the corresponding chlorido complex. A similar trend was observed for closely related studies performed by Bugarčić and co-workers before.[44,46−48]

A few of the studied substitution reactions were also investigated as a function of temperature. According to the results given in Table 3, the large sensitivity of the rate constants for the σ-donor properties of the entering ligands is in line with an associative substitution mode. The significantly negative values for the entropy of activation confirm the associative (A or I_a) character of the substitution process. In addition, the reaction between $[Pd(tpdm)Cl]^+$ and glutathione was studied as a function of pressure, and the obtained volume of activation further supports the associative nature of the substitution process.

During the past few decades many scientists have investigated the interaction between Pt(II) complexes and different biologically relevant ligands. Very important results were observed for some monofunctional Pt(II) complexes, which contain NNN tridentate ligands. These complexes are interesting because their behavior depends strongly on the structure of the tridentate ligands. For example, in the case of the terpy chelate, there is strong interaction between the metal ion and the pyridine rings, especially with the central pyridine ring in the terpy chelate, which results in a strong trans effect and very fast substitution reactions.[11a,b] In the case of the other tridentate NNN ligands the presence and position of the pyridine rings have a large influence on the behavior of the complex.

dx.doi.org/10.1021/ic201807a | Inorg. Chem. 2012, 51, 1516−1529

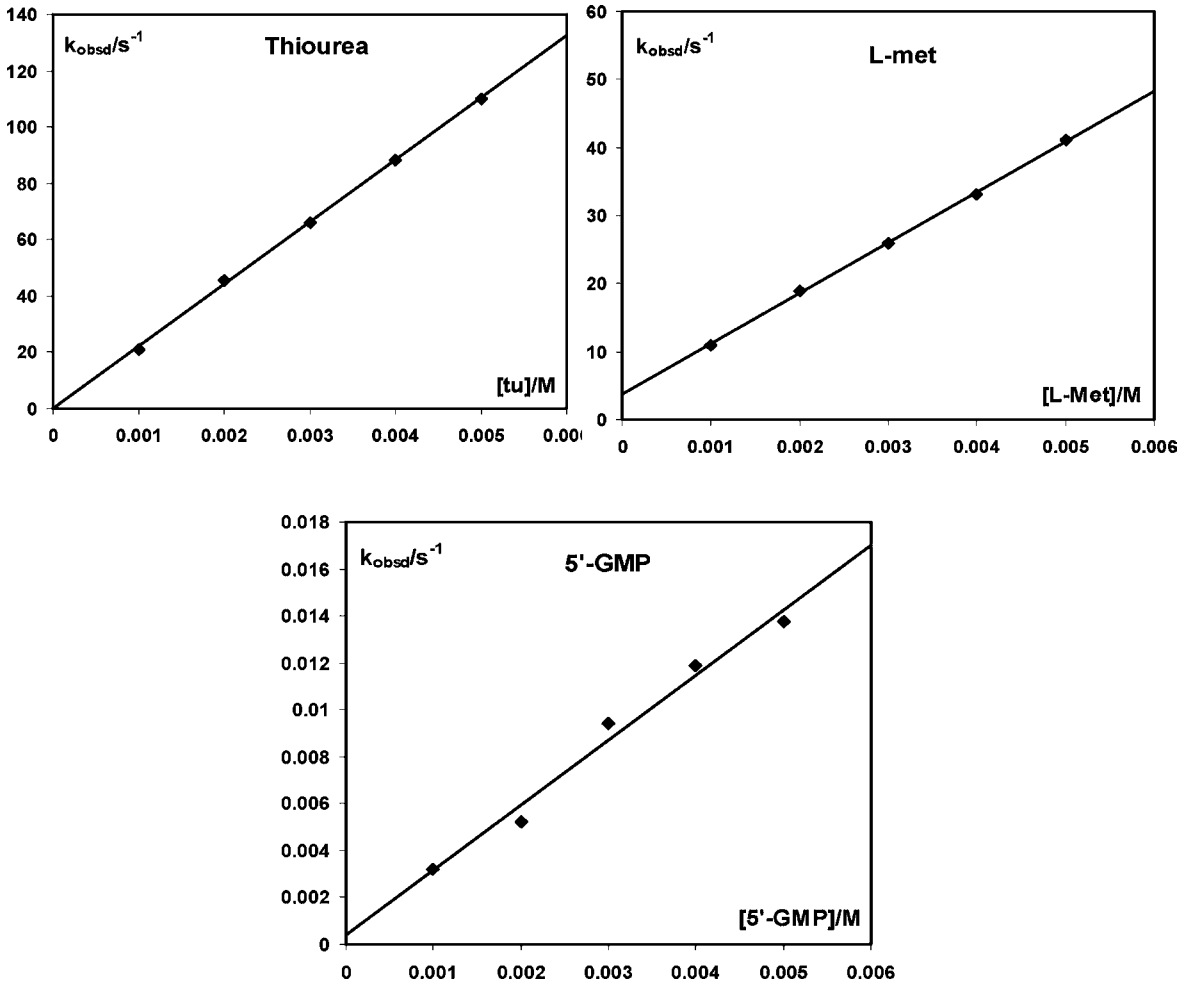

Figure 7. Pseudo-first-order rate constants, k_{obsd}, as a function of entering nucleophile concentration for substitution reactions of $[Pd(tpdm)(H_2O)]^{2+}$ at 298 K in 0.1 M $NaClO_4$ and pH = 2.5.

In general, we can conclude that the reactivity of the employed nucleophiles toward novel monofunctional complexes of Pt(II) and Pd(II) follow the same order as was found, for example, for the corresponding dien, bpma, and terpy complexes. However, on comparing the rate constants, large differences are observed.

In Table 4 the published data for k_2 for substitution of some Pt(II) chlorido complexes are compared for terpy, bpma, and dien. From this data it follows that the terpy complex is more reactive than the bpma complex, whereas the dien complex has the lowest reactivity of all. The $[Pt(tpdm)Cl]^+$ complex studied here is almost as reactive as the dien complex. This clearly illustrates that a relatively small structural modification of the tridentate ligand has a strong influence on the reactivity of the complex.

Computational Studies. A comparison of the computed structures (B3LYP/LANL2DZp) for $[Pt(terpy)Cl]^+$ and $[Pt(tpdm)Cl]^+$ reveals one strongly differing bond, viz. the N_{Py}–Pt bond trans to Pt–Cl. While the *cis*-N_{Py}–Pt bonds in the terpy and tpdm complexes differ only by 0.01 Å, a significant change is observed for the *trans*-N_{Py}–Pt bond (see Figure 9). Because of the different structural necessities of the chelate rings, viz. six membered in $[Pt(tpdm)Cl]^+$ and five-membered in $[Pt(terpy)Cl]^+$, the ring strain influences the *trans*-N_{Py}–Pt bond very strongly, leading to a 0.1 Å longer bond in $[Pt(tpdm)Cl]^+$ (2.06 Å) than in $[Pt(terpy)Cl]^+$ (1.96 Å).

The influence of the chelate ring size can also be seen in the angles at the Pt center. Whereas in $[Pt(terpy)Cl]^+$ the N_{Py}–Pt–N_{Py} angle is 81.0° and the N_{Py}–Pt–Cl angle has to be 99.0°, in $[Pt(tpdm)Cl]^+$ the N_{Py}–Pt–N_{Py} angle of 89.3° and the N_{Py}–Pt–Cl angle of 90.7° are nearly identical for a square-planar Pt(II) center. Furthermore, $[Pt(terpy)Cl]^+$ has a perfect planar structure, whereas $[Pt(tpdm)Cl]^+$ is highly distorted. Besides the electronic influences of the tpdm ligand, this distortion is another reason for the lower reactivity of $[Pt(tpdm)Cl]^+$ as the attack of a nucleophile on the Pt(II) center is hindered as shown in Figure 9, and even the final coordination to the Pt(II) center is hindered as shown by the elongated Pt–Cl bond (0.06 Å) and the shortened H_{Py}–Cl contact (−0.04 Å) (see Figure 9).

To learn more about the possible stability differences on coordinating S-donor ligands to the $[Pt(terpy)Cl]^+$ or $[Pt(tpdm)Cl]^+$ fragments, we studied the following reactions

$$[Pt(terpy)Cl]^+ + Tu \rightarrow [Pt(terpy)Tu]^{2+} + Cl^-$$

$$\text{B3LYP(CPCM)/LANL2DZp//B3LYP/LANL2DZp: } -44.3 \text{ kJ mol}^{-1}$$

$$Pt(tpdm)Cl]^+ + Tu \rightarrow [Pt(tpdm)Tu]^{2+} + Cl^-$$

$$\text{B3LYP(CPCM)/LANL2DZp//B3LYP/LANL2DZp: } -46.4 \text{ kJ mol}^{-1}$$

dx.doi.org/10.1021/ic201807a | *Inorg. Chem.* 2012, 51, 1516–1529

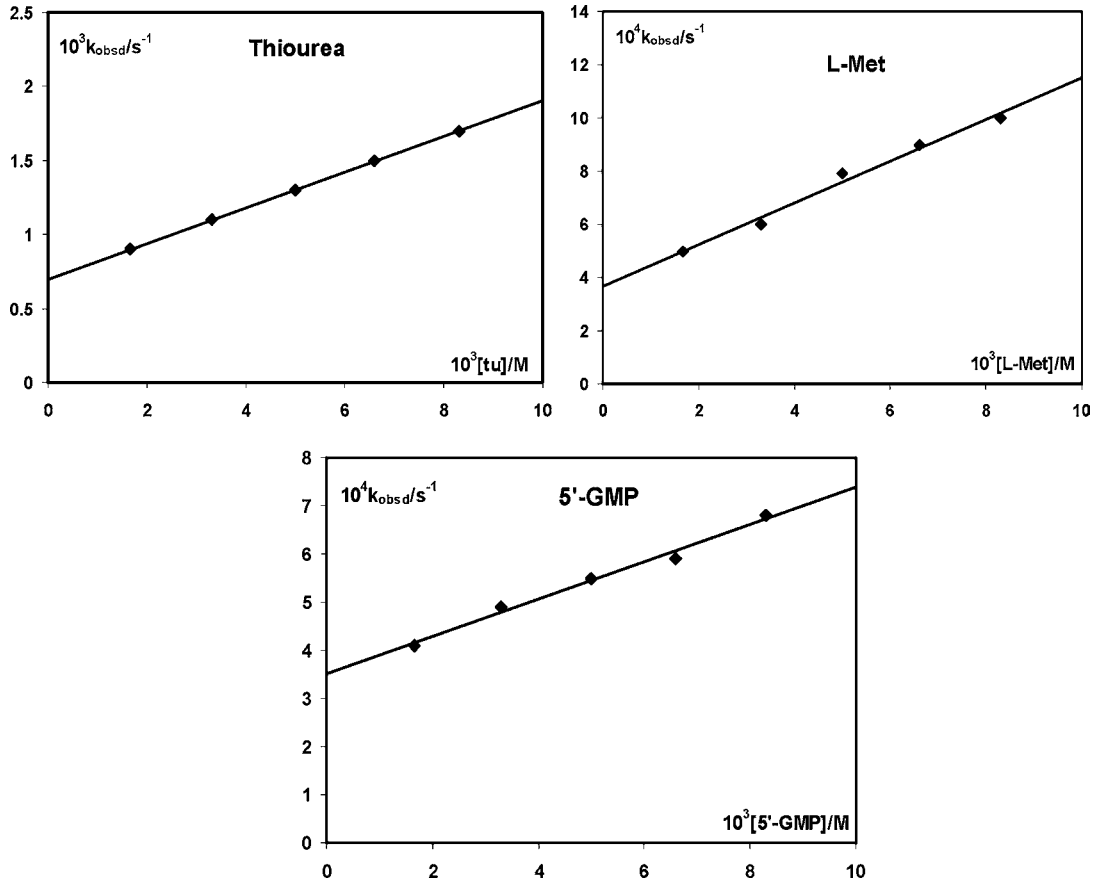

Figure 8. Pseudo-first-order rate constants, k_{obsd}, as a function of entering nucleophile concentration for substitution reactions of $[Pt(tpdm)(H_2O)]^{2+}$ at 298 K in 0.1 M $NaClO_4$ and pH = 2.5.

Table 4. Rate Constants for Substitution Reactions of Some Pt(II) Complexes with tu, L-met, GSH, and 5′-GMP

complex	ligand	$k_2/M^{-1}\ s^{-1}$	ref
$[Pt(tpdm)Cl]^+$	thiourea	$(12.1 \pm 0.1) \times 10^{-2}$	this work
	L-met	$(6.21 \pm 0.05) \times 10^{-2}$	this work
	GSH	$(1.79 \pm 0.01) \times 10^{-2}$	this work
	5′-GMP	$(1.63 \pm 0.04) \times 10^{-2}$	this work
$[Pt(terpy)Cl]^+$	thiourea	$(1.52 \pm 0.48) \times 10^{4}$	41
	GSH	$(1.32 \pm 0.48) \times 10^{3}$	41
	5′-GMP	$(1.98 \pm 0.08) \times 10^{2}$	41
$[Pt(bpma)Cl]^+$	L-met	0.14 ± 0.01	43
	GSH	$(4.1 \pm 0.1) \times 10^{-2}$	43
	5′-GMP	$(5.48 \pm 0.06) \times 10^{-2}$	43
$[Pt(dien)Cl]^+$	L-Met	$(7.2 \pm 0.3) \times 10^{-2}$	45
	GSH	$(3.0 \pm 0.2) \times 10^{-2}$	45
	5′-GMP	$(1.91 \pm 0.06) \times 10^{-2}$	45

The CPCM energy computations show almost identical values for the terpy and tpdm complexes. Therefore, the origin of the lower reactivity of $[Pt(tpdm)Cl]^+$ has to be attributed to transition state effects and not to the better complexation properties of the product.

The enhanced π-accepting ability of the terpy chelate as compared to tpdm is supported by the computational analysis performed on the corresponding Ni(II) complexes summarized in Figures 10 and 11. The delocalization energy resulting from the interaction between the terpy ligand and the metal center was evaluated by comparing the energy of the standard complex (**A**) with that of the structure in which the delocalization from the metal toward the ligand is switched off (**B**). A value of 69.9 kJ mol^{-1} was obtained, but a slightly higher value of 77.9 kJ mol^{-1} can be derived by comparing **C** and **G**, in which the delocalization between the rings is also interrupted. A more detailed analysis of the contributions of each individual rings **D** vs **H** and **E** vs **I** suggest that 50% of the effect (~42 kJ mol^{-1}) comes from the central ring.

The $NICS_{\pi zz}$ computations on the same electronic states corroborated the conclusions based on the delocalization energies and show that the outer rings in **A** are more weakly affected by the π-back-donation from the metal than the central ring: switching the π-back-donation off (as in **B**) does not alter the aromaticity of the ring significantly ($NICS_{\pi zz}$ values vary from −29.1 to −28.7 ppm), whereas the aromaticity of the inner ring is reduced when the interaction with the ring is switched off (from −24.4 to −22.6 ppm). The central ring might thus benefit the most from the electronic delocalization from the metal. Note that if the conjugation between the rings reduces the aromaticity of each individual ring (e.g., −29.1/−24.4 ppm in **A** and −34.0/−33.4 ppm in **C**), the effect is not a property of only the complex but also observed in the free ligand (constrain to a planar geometry, see **F** vs **G**).

As compared to $[Ni(terpy)Cl]^+$, the number of blocking patterns for $[Ni(tpdm)Cl]^+$ is reduced due to the nonplanarity of the ligand: the π bonds can only be blocked for one ring at a time. In sharp contrast with $[Ni(terpy)Cl]^+$, the delocalization energy resulting from the interaction between the central ring and the metal in $[Ni(tpdm)Cl]^+$ is zero (see Figure 11).

dx.doi.org/10.1021/ic201807a | Inorg. Chem. 2012, 51, 1516−1529

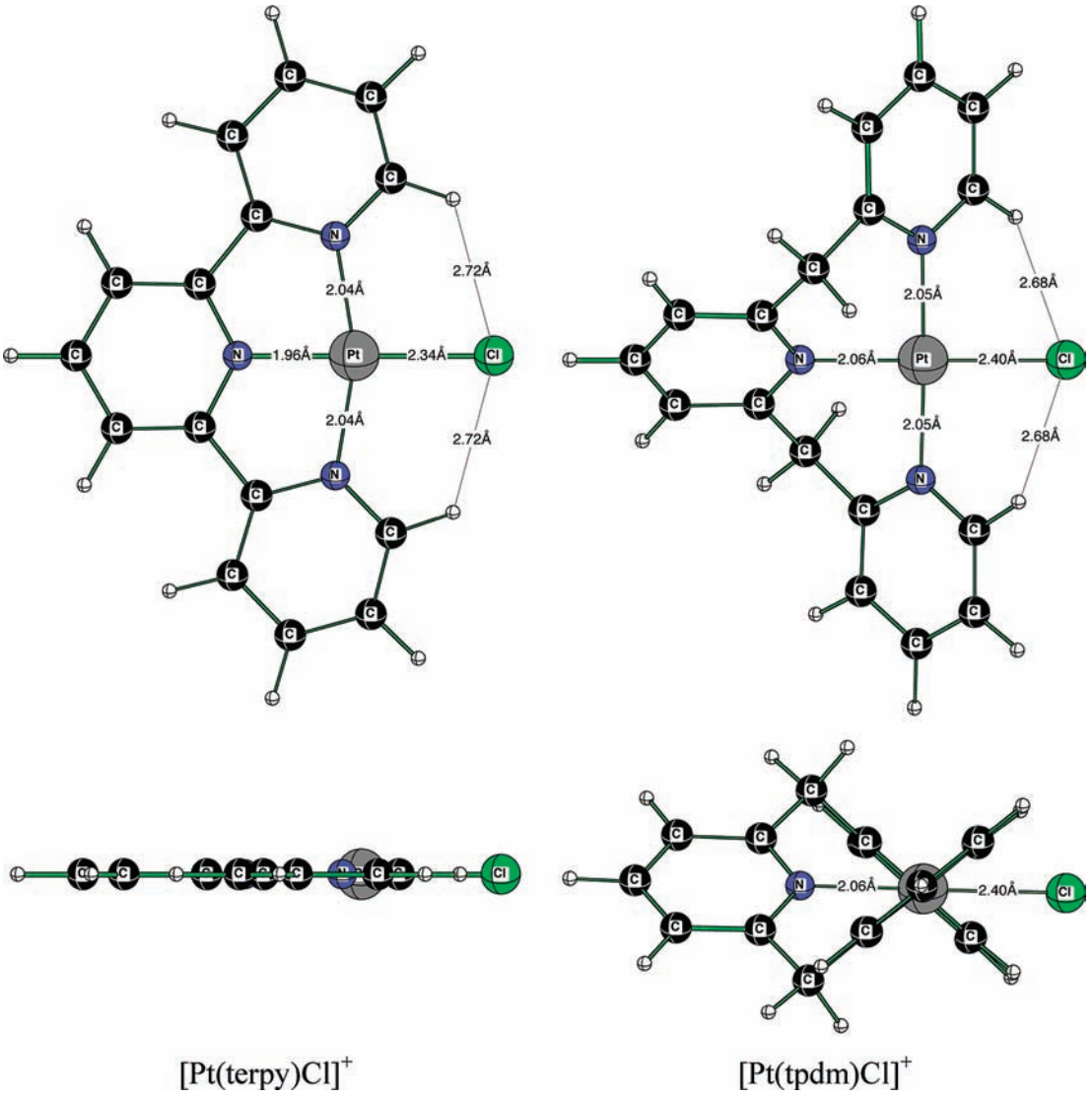

Figure 9. Computed structures (B3LYP/LANL2DZp) of $[Pt(terpy)Cl]^+$ and $[Pt(tpdm)Cl]^+$.

The free ligand with the central ring blocked **O** and its analogue complex structure **L** are both characterized by the same delocalization energy (~55 kJ mol^{-1}). The delocalization between the outer ring and the metal is more significant (at least 49.4 − 32.2 = 17.2 kcal mol^{-1} when comparing **K** and **N**), but the energetic effects are still considerably smaller than those computed for the terpy ligand. Detailed comparisons of the $NICS_{\pi zz}$ values between **J** and **K** reveal that the π charge transfer from the transition metal enhances the aromaticity of the terminal ring (−34.3 ppm in **J** vs −29.8 ppm in **K**). Most of this difference arises from the lack of interaction between the rings in **K** (see the difference between the outer ring between **N** and **M** in the free ligand), but a small remaining fraction (1 ppm) can be attributed to the π charge transfer. A similar effect is observed for the central ring (**J** and **L**). The aromaticity is enhanced when the π-back-donation is enabled but by only 1 ppm (the rest being due to the delocalization between the ring, see **M** and **O**). These magnetic changes are slightly stronger than that affecting the outer ring of the terpy ligand but not as strong as for the inner ring of the preceding complex.

Note that if one can easily understand the existence of an electron delocalization between the three parallel aromatic rings in the terpy ligand, tdpm is not planar, and thus, the aromaticity difference between the rings in **M**, **N**, and **O** is perhaps less obvious to interpret. The situation is in fact very similar to the cyclopentadiene molecule in which the π orbitals overlap occurs through the pseudo-sp^2 methylene carbons. As mentioned earlier, the aromaticity of the individual ring in the tpdm complex is reduced when the rings do not interact (compare **J**/**M** with **K**/**N** and **L**/**O**), in contrast with the terpy case. This effect, which is also true for the free ligand, further illustrates the contrasting electronic properties of the two ligands. As the observed differences between the two complexes are intimately connected to the intrinsic electronic properties of the ligands, we can thus expect that similar contrasts would affect their respective transition state and hence the reaction rate.

In summary, for the terpy complexes, the outer rings are not affected by the π-back-donation but the inner ring is more aromatic when the π charge transfer is present (by a significant amount of 2 ppm). From the energetic aspect, the electronic delocalization between the metal and the ligand is equal to 67 kJ mol^{-1} and can account for the huge acceleration of the nucleophilic substitution process due to the increase in the electrophilicity of the metal center.

dx.doi.org/10.1021/ic201807a | *Inorg. Chem.* 2012, 51, 1516−1529

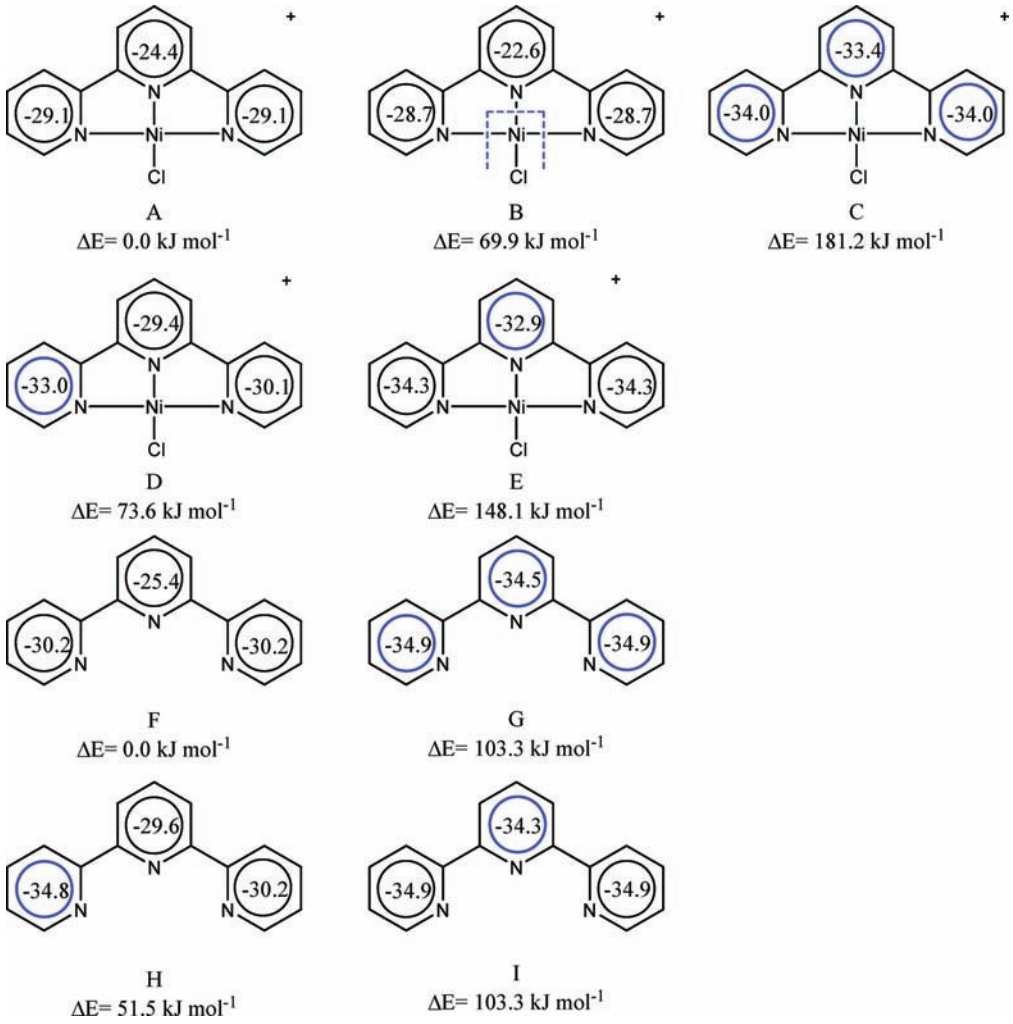

Figure 10. terpy complexes and their BLW structures. Blocking scheme in the top middle figure symbolizes a completely delocalized ligand but no π charge transfer from/to the metal. Delocalization energies (E(BLW) − E(canonical)) are given below each individual structure.

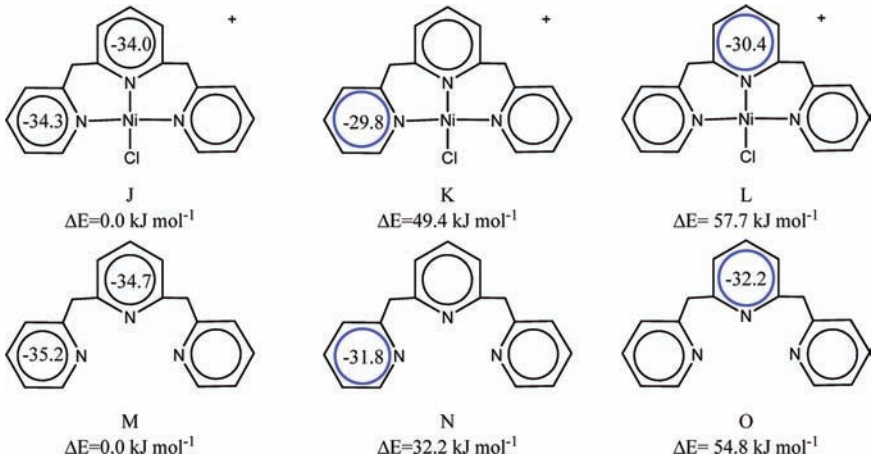

Figure 11. tpdm complexes and their BLW structures. ΔE indicates the delocalization energy.

CONCLUSIONS

This investigation demonstrated the relation between the structure and the reactivity of Pd(II) and Pt(II) complexes with chelating ligands containing the pyridine moiety. These complexes are very interesting because their behavior strongly depends on the structure of the tridentate ligands. In their structure the pyridine rings in the tridentate tpdm ligand are separated by methylene groups, so the system is more flexible in comparison with terpyridine, which is confirmed by the crystal structure of the [Pt(tpdm)Cl]Cl complex. This higher flexibility enables the substitution reaction with thioether L-methionine. The computational studies have clearly demonstrated that the

dx.doi.org/10.1021/ic201807a | Inorg. Chem. 2012, 51, 1516−1529

π-back-bonding properties of the terpy chelate can account for the acceleration of the nucleophilic substitution process as compared to the tpdm chelate where introduction of two methylene groups prevents such an effective π-back-bonding. The DFT (B3LYP/LANL2DZp) computations confirmed the reactivity toward thioethers. The results observed for substitution reactions of monofunctional $[Pt(tpdm)Cl]^+$ and $[Pd(tpdm)Cl]^+$ complexes and their aqua analogues with the biologically relevant nucleophiles thiourea, L-methionine, glutathione, and guanosine-5′-monophosphate have shown the higher reactivity of Pd(II) complexes as well as the higher reactivity for aqua complexes than the corresponding chlorido complexes. Also, the associative mode of substitution was confirmed for all studied reactions.

■ ASSOCIATED CONTENT

Supporting Information

Observed pseudo-first-order rate constants as a function of entering nucleophile concentration and temperature for substitution reactions of $[Pd(tpdm)Cl]^+$, $[Pd(tpdm)(H_2O)]^{2+}$, $[Pt(tpdm)Cl]^+$, and $[Pt(tpdm)(H_2O)]^{2+}$ in 0.10 M $NaClO_4$, pH = 2.5, and 10 mM NaCl (Tables S1–S7); observed pseudo-first-order rate constants as a function of NaCl concentration for substitution reaction of $[Pd(tpdm)(H_2O)]^{2+}$ with thiourea in 0.10 M $NaClO_4$ at pH = 2.5 (Table S8); observed pseudo-first-order rate constants as a function of pressure for substitution reactions of $[Pd(tpdm)Cl]^+$ with glutathione in 0.10 M $NaClO_4$, pH = 2.5, 10 mM NaCl, $[GSH] = 2 \times 10^{-3}$ M, and 283 K (Table S9); hydrogen-bond parameters for $[Pt(tpdm)Cl]Cl\cdot 1.25H_2O$ (Table S10); UV–vis and IR spectra of the $[Pt(tpdm)Cl]Cl$ compound (Figures S1 and S2); UV–vis and IR spectra of the $[Pd(tpdm)Cl]Cl$ compound (Figures S3 and S4); UV–vis and IR spectra of the $[Pt(tpdm)(H_2O)]^{2+}$ complex (Figures S5 and S6); UV–vis and IR spectra of the $[Pd(tpdm)(H_2O)]^{2+}$ complex (Figures S7 and S8); UV–vis spectra recorded for reaction between $[Pd(tpdm)Cl]^+$ and thiourea; UV–vis spectra recorded for reaction between $[Pd(tpdm)Cl]^+$ and thiourea (Figures S9); UV–vis spectra recorded for reaction between $[Pt(tpdm)Cl]^+$ and 5′-GMP (Figure S10); UV–vis spectra recorded for reaction between $[Pt(tpdm)(H_2O)]^{2+}$and 5′-GMP (Figures S11); UV–vis spectra recorded for reaction between $[Pt(tpdm)(H_2O)]^{2+}$and thiourea (Figure S12). This material is available free of charge via the Internet at http://pubs.acs.org.

■ AUTHOR INFORMATION

Corresponding Author

*E-mail: bugarcic@kg.ac.rs (Z.D.B.); vaneldik@chemie.uni-erlangen.de (R.v.E.).

■ ACKNOWLEDGMENTS

The authors gratefully acknowledge financial support from DAAD, the Deutsche Forschungsgemeinschaft, and the Ministry of Science and Technological Development of the Republic of Serbia, project No. 172011. We would like to thank Prof. Tim Clark for hosting this work in the CCC and the Regionales Rechenzentrum Erlangen (RRZE) for a generous allotment of computer time. C.C. and S.N.S. acknowledge the Sandoz family foundation, the Swiss NSF grant 200021-121577/1, and EPFL for financial support.

■ REFERENCES

(1) Vicente, J.; Arcas, A. *Coord. Chem. Rev.* **2005**, *249*, 1135–115.
(2) Hubbard, C. D.; van Eldik, R. *J. Coord. Chem.* **2007**, *60*, 1–51.
(3) Hambley, T. W. *Science* **2007**, *318*, 1392–1393.
(4) Kelland, L. *Nat. Rev. Cancer* **2007**, *7*, 573–584.
(5) van Rijt, S. H.; Sadler, P. J. *Drug Discovery Today* **2009**, *23/24*, 1089–1097.
(6) Lovejoy, K. S.; Lippard, S. J. *Dalton Trans.* **2009**, 10651–10659.
(7) In *Bioinorganic Medicinal Chemistry*; Alessio, E., Ed.; Wiley-VCH: Weinheim, 2011.
(8) (a) Reedijk, J. *Platinum Met. Rev.* **2008**, *52*, 2–11. (b) Reedijk, J. *Eur. J. Inorg. Chem.* **2009**, *10*, 1303–1312.
(9) Rau, T.; van Eldik, R. In *Metal Ions in Biological Systems*; Sigel, A., Sigel, H., Eds.; Marcel Dekker: New York, 1996; Vol. *32*, pp 340–378.
(10) (a) Breet, E. L. J.; van Eldik, R. *Inorg. Chem.* **1984**, *23*, 1865–1869. (b) Kotowski, M.; van Eldik, R. *Inorg. Chem.* **1984**, *23*, 3310–3312. (c) Kotowski, M.; van Eldik, R. *Inorg. Chem.* **1986**, *25*, 3896–3899. (d) Pienaar, J. J.; Kotowski, M.; van Eldik, R. *Inorg. Chem.* **1989**, *28*, 373–375. (e) Berger, J.; Kotowski, M.; van Eldik, R.; Frey, U.; Helm, L.; Merbach, A. E. *Inorg. Chem.* **1989**, *28*, 3759–3765.
(11) (a) Jaganyi, D.; Hofmann, A.; van Eldik, R. *Angew. Chem., Int. Ed.* **2001**, *40*, 1680–1683. (b) Hofmann, A.; Jaganyi, D.; Munro, O. Q.; Liehr, G.; van Eldik, R. *Inorg. Chem.* **2003**, *42*, 1688–1700. (c) Bugarčić, Ž. D.; Liehr, G.; van Eldik, R. *Dalton Trans.* **2002**, 951–956. (d) Bugarčić, Ž. D.; Petrović., B. V.; Zangrando, E. *Inorg. Chim. Acta* **2004**, *357*, 2650–2656. (e) Jaganyi, D.; Tiba, F.; Munro, O. Q.; Petrović, B.; Bugarčić, Ž. D. *Dalton Trans.* **2006**, 2943–2946. (f) Bugarčić, Ž. D.; Liehr, G.; van Eldik, R. *Dalton Trans.* **2002**, 2825–2830. (g) Jaganyi, D.; Reddy, D.; Gertenbach, J. A.; Hofmann, A.; van Eldik, R. *Dalton Trans.* **2004**, 299–304.
(12) Schiessl, W. C.; Summa, N. K.; Weber, C. F.; Gubo, S.; Dücker-Benfer, C.; Puchta, R.; van Eikema Hommes, N. J. R.; van Eldik, R. *Z. Anorg. Allg. Chem.* **2005**, *631*, 2812–2819.
(13) Ashby, M. T. *Comments Inorg. Chem.* **1990**, *10*, 297–313.
(14) Murray, S. G.; Hartley, F. R. *Chem. Rev.* **1981**, *81*, 365–414.
(15) Vedernikov, A. N.; Huffman, J. C; Caulton, K. G. *Inorg. Chem.* **2002**, *41*, 6244–6248.
(16) Appleton, T. G.; Hall, J. R.; Ralph, S. F.; Thompson, C. S. M. *Inorg. Chem.* **1984**, *23*, 3521–3525.
(17) van Eldik, R.; Gaede, W.; Wieland, S.; Kraft, J.; Spitzer, M.; Palmer, D. A. *Rev. Sci. Instrum.* **1993**, *64*, 1355–1357.
(18) (a) Becke, A. D. *J. Phys. Chem.* **1993**, *97*, 5648–5652. (b) Lee, C.; Yang, W.; Parr, R. G. *Phys. Rev. B* **1988**, *37*, 785–789. (c) Stephens, P. J.; Devlin, F. J.; Chabalowski, C. F.; Frisch, M. J. *J. Phys. Chem.* **1994**, *98*, 11623–11627. (d) Dunning, T. H. Jr.; Hay, P. *J. Mod. Theor. Chem* **1976**, *3*, 1–28. (e) Hay, P. J.; Wadt, W. R. *J. Chem. Phys.* **1985**, *82*, 270–283. (f) Hay, P. J.; Wadt, W. R. *J. Chem. Phys.* **1985**, *82*, 284–298. (g) Hay, P. J.; Wadt, W. R. *J. Chem. Phys.* **1985**, *82*, 299–310. (h) In *Gaussian Basis Sets for Molecular Calculations*; Huzinaga, S., ed.; Elsevier: Amsterdam, 1984.
(19) The performance of the computational level employed in this study is well documented, see, for example: (a) Puchta, R.; Meier, R.; van Eikema Hommes, N. J. R.; van Eldik, R. *Eur. J. Inorg. Chem.* **2006**, 4063–4067. (b) Scheurer, A.; Maid, H.; Hampel, F.; Saalfrank, R. W.; Toupet, L.; Mosset, P.; Puchta, R.; van Eikema Hommes, N. J. R. *Eur. J. Org. Chem.* **2005**, 2566–2574. (c) Illner, P.; Zahl, A.; Puchta, R.; van Eikema Hommes, N.; Wasserscheid, P.; van Eldik, R. *J. Organomet. Chem.* **2005**, *690*, 3567–3576. (d) Weber, C. F.; Puchta, R.; van Eikema Hommes, N.; Wasserscheid, P.; van Eldik, R. *Angew. Chem.* **2005**, *117*, 6187–6192. (e) Weber, F.; Puchta, R.; van Eikema Hommes, N.; Wasserscheid, P.; van Eldik, R. *Angew. Chem., Int. Ed.* **2005**, *44*, 6033–6038. (f) Puchta, R.; Dahlenburg, L.; Clark, T. *Chem.—Eur. J.* **2008**, *14*, 8898–8903. (g) Illner, P.; Begel, S.; Kern, S.; Puchta, R.; van Eldik, R. *Inorg. Chem.* **2009**, *48*, 588–597. (h) Alzoubi, B. M.; Vidali, F.; Puchta, R.; Dücker-Benfer, C.; Felluga, A.; Randaccio, L.; Tauzher, G.; van Eldik, R. *Dalton Trans.* **2009**, 2392–2399. (i) Soldatović, T.; Shoukry, M.; Puchta, R.; Bugarčić, Ž. D.; van Eldik, R. *Eur. J. Inorg. Chem.* **2009**, 2261–2270 and literature cited therein.

(20) Frisch, M. J.; Trucks, G. W.; Schlegel, H. B.; Scuseria, G. E.; Robb, M. A.; Cheeseman, J. R.; Montgomery, Jr., J. A.; Vreven, T.; Kudin, K. N.; Burant, J. C.; Millam, J. M.; Iyengar, S. S.; Tomasi, J.; Barone, V.; Mennucci, B.; Cossi, M.; Scalmani, G.; Rega, N.; Petersson, G. A.; Nakatsuji, H.; Hada, M.; Ehara, M.; Toyota, K.; Fukuda, R.; Hasegawa, J.; Ishida, M.; Nakajima, T.; Honda, Y.; Kitao, O.; Nakai, H.; Klene, M.; Li, X.; Knox, J. E.; Hratchian, H. P.; Cross, J. B.; Bakken, V.; Adamo, C.; Jaramillo, J.; Gomperts, R.; Stratmann, R. E.; Yazyev, O.; Austin, A. J.; Cammi, R.; Pomelli, C.; Ochterski, J. W.; Ayala, P. Y.; Morokuma, K.; Voth, G. A.; Salvador, P.; Dannenberg, J. J.; Zakrzewski, V. G.; Dapprich, S.; Daniels, A. D.; Strain, M. C.; Farkas, O.; Malick, D. K.; Rabuck, A. D.; Raghavachari, K.; Foresman, J. B.; Ortiz, J. V.; Cui, Q.; Baboul, A. G.; Clifford, S.; Cioslowski, J.; Stefanov, B. B.; Liu, G.; Liashenko, A.; Piskorz, P.; Komaromi, I.; Martin, R. L.; Fox, D. J.; Keith, T.; Al-Laham, M. A.; Peng, C. Z.; Nanayakkara, A.; Challacombe, M.; Gill, P. M. W.; Johnson, B.; Chen, W.; Wong, M. W.; Gonzalez, C.; Pople, J. A. *Gaussian 03*, Revision B.03; Gaussian Inc.: Wallingford, CT, 2004.
(21) (a) Barone, V.; Cossi, M. *J. Phys. Chem. A* **1998**, *102*, 1995−2001. (b) Cossi, M.; Scalmani, G.; Rega, N.; Barone, V. *J. Comput. Chem.* **2003**, *24*, 669−796.
(22) Steinmann, S. N.; Jana, D. F.; Wu, J. I.-C.; Schleyer, P. v. R.; Mo, Y.; Corminboeuf, C. *Angew. Chem., Int. Ed.* **2009**, *48*, 9828−9833.
(23) Mo, Y.; Peyerimhoff, S. D. *J. Chem. Phys.* **1998**, *109*, 1687−1697.
(24) Mo, Y.; Song, L.; Lin, Y. *J. Phys. Chem. A* **2007**, *111*, 8291−8301.
(25) Kutzelnigg, W. *Isr. J. Chem.* **1980**, *19*, 193.
(26) (a) Schleyer, P. v. R.; Maerker, C.; Dransfeld, A.; Jiao, H. J.; Hommes, N. J. R. V. *J. Am. Chem. Soc.* **1996**, *118*, 6317−6318. (b) Schleyer, P v. R.; Jiao, H.; Hommes, N. J. R. v. E.; Malkin, V. G.; Malkina, O. L. *J. Am. Chem. Soc.* **1997**, *119*, 12669−12670. (c) Schleyer, P. v. R.; Manoharan, M.; Wang, Z.-X.; Kiran, B.; Jiao, H.; Puchta, R.; Hommes, N. J. R. v. E. *Org. Lett.* **2001**, *3*, 2465−2465. (d) Chen, Z.; Wannere, C. S.; Corminboeuf, C.; Puchta, R.; Schleyer, P. v. R. *Chem. Rev.* **2005**, *105*, 3842−3888.
(27) Corminboeuf, C.; Heine, T.; Seifert, G.; Schleyer, P. v. R.; Weber, J. *Phys. Chem. Chem. Phys.* **2004**, *6*, 273−276.
(28) Schmidt, M. W.; Baldridge, K. K.; Boatz, J. A.; Elbert, S. T.; Gordon, M. S.; Jensen, J. H.; Koseki, S.; Matsunaga, N.; Nguyen, K. A.; Su, S.; Windus, T. L.; Dupuis, M.; Montgomery, J. A. Jr. *J. Comput. Chem.* **1993**, *14*, 1347−1363.
(29) In *Theory and Applications of Computational Chemistry: The First Forty Years*; Gordon, M. S., Schmidt, M. W., Eds.; Elsevier: Amsterdam, 2005.
(30) Malkin, V. G.; Malkina, O. L.; Casida, M. E.; Salahub, D. R. *J. Am. Chem. Soc.* **1994**, *116*, 5898−5908.
(31) Malkin, V. G.; Malkina, O. L.; Salahub, D. R. *Chem. Phys. Lett.* **1993**, *204*, 87−95.
(32) Perdew, J. P.; Chevary, J. A.; Vosko, S. H.; Jackson, K. A.; Pederson, M. R.; Singh, D. J.; Fiolhais, C. *Phys. Rev. B* **1992**, *46*, 6671.
(33) Murray, C. W.; Handy, N. C.; Laming, G. J. *Mol. Phys.* **1993**, *78*, 997−1014.
(34) Lebedev, V. I.; Laikov, D. N. *Dokl. Math.* **1999**, *59*, 477−481.
(35) (a) Wong, Y. S.; Y., S.; Lippard, S. J. *J. Chem. Soc., Chem. Commun.* **1977**, 824−825. (b) Sengul, A. *Turk. J. Chem.* **2004**, *28*, 667−672. (c) Jennette, K. W.; Gill, J. T.; Sadownick, J. A.; Lippard, S. J. *J. Am. Chem. Soc.* **1976**, *98*, 6159−6168.
(36) Tobe, M. L.; Burgess, J. *Inorganic Reaction Mechanisms*: Addision Wesley Longman: Harlow, 1999; Chapter 3.
(37) Annibale, G.; Brandolisio, M.; Bugarčić, Ž. D.; Cattalini, L. *Transition Met. Chem* **1998**, *23*, 715−719.
(38) Zhou, X, Y.; Kostic, N. M. *Polyhedron* **1990**, *9*, 1975−1983.
(39) Smith, R. M.; Martel, A. E. *Critical Stability Constants*; Plenum Press: New York, 1989; Vol. *6*, 2nd Suppl., p 20.
(40) Bugarčić, Ž. D.; Jančić, D. M.; Shoukry, A. A.; Shoukry, M. M. *Monatsh. Chem.* **2004**, *135*, 151−160.
(41) Petrović, D.; Stojimirović, B.; Petrović, B.; Bugarčić, Z. M.; Bugarčić, Ž. D. *Bioorg. Med. Chem.* **2007**, *15*, 4203−4211.
(42) Vasić, V.; Čakar, M.; Savić, J.; Petrović, B.; Nedeljković, J.; Bugarčić, Ž. D. *Polyhedron* **2003**, *22*, 279−284.
(43) Bugarčić, Ž. D.; Rosić, J.; Petrović, B.; Summa, N.; Puchta, R.; van Eldik, R. *J. Biol. Inorg. Chem.* **2007**, *12*, 1141−1150.
(44) Soldatović, T.; Bugarčić, Ž. D. *J. Inorg. Biochem.* **2005**, *99*, 1472−1479.
(45) Soldatović, T.; Vasić, V.; Bugarčić, Ž. D. *Bull. Chem. Soc. Jpn.* **2006**, *79*, 1889−1893.
(46) Rosic, J.; Petrović, B.; Djuran, M. I.; Bugarčić, Z. D. *Monatsh. Chem.* **2007**, *138*, 1−11.
(47) Petrović, B.; Bugarčić, Z. D. *Austral. J. Chem.* **2005**, *7*, 544−550.
(48) Petrović, B.; Djuran, M. I.; Bugarčić, Z. D. *Met. Based Drugs* **1999**, *6*, 355−362.